LECTURE NOTES

John V. Breakwell, Professor
Department of Aeronautics & Astronautics
Stanford University
Stanford, California 94305/USA

A GENERAL PROBLEM

Given $\begin{cases} n \times 1 \\ \dot{x} = f(x,u,v) \\ \text{initial state } x_0 \end{cases}$, $\begin{cases} u \in U \\ v \in V \end{cases}$,

where the control sets U, V are independent of the state x, find the control histories u,v to be chosen by players 1 and 2, so as to minimize and maximize respectively the value of a certain function $M(x_f)$ of the "terminal state" x_f at the moment t_f when the state reaches a certain "terminal manifold" $C(x) = 0$. (Let us assume that all possible paths reach this terminal manifold in finite time.)

OUTLINE OF THE SOLUTION

Let $J(x)$ denote the value of $M(x_f)$ resulting from "optimal play" by both players when the initial state is x. Then (this is Isaacs' "main equation")

$$0 = \min_{u\in U} \max_{v\in V} J_x f(x,u,v) \left[= \min_{u\in U} \max_{v\in V} \frac{dJ}{dt} \right] \qquad (1)^{\ddagger}$$

thereby defining optimal controls (not necessarily unique) in the "closed-loop" form $u = u^*(x)$, $v = v^*(x)$. The optimality is an immediate consequence of (1): Player 1 by using $u^*(x)$, can prevent the path from moving off of the surface $J(x) = J(x_0)$ towards higher J-values; hence he can prevent $M(x_f)$ from exceeding $J(x_0)$. Similarly, player 2, by using $v^*(x)$, can prevent $M(x_f)$ from falling below $J(x_0)$. The determination of the optimal controls $u^*(x)$, $v^*(x)$ rests on the solution of the partial D.E. (1) for the function $J(x)$, subject to $J(x) = M(x)$ on $C(x) = 0$.

Suppose now that $J(x)$ is twice-differentiable inside some region $\mathcal{R}$. Partial differentiation of (1) w.r.t. x at any point in the interior of $\mathcal{R}$ shows that

$$0 = J_{xx} f(x,u^*(x),v^*(x)) + J_x (f_x + f_u u^*_x + f_v v^*_x) \quad .$$

But $J_x f_u u^*_x = J_x f_v v^*_x = 0$, whether or not $u^*(x)$, $v^*(x)$ lie on the boundaries of sets U, V. Hence

$$\dot{J}_x \left(= J_{xx} f \right) = - J_x f_x \quad , \qquad (2)$$

as long as the optimal path remains in the interior of $\mathcal{R}$.

If $C(x) = 0$ is a smooth (n-1)-dimensional manifold, the terminal gradient $J_x(x_f)$ at any x_f is uniquely determined by (1) together with $J(x) = M(x)$ on $C(x) = 0$. The "adjoint equations" (2) may be integrated backwards from t_f along with the path equations $\dot{x} = f(x,u^*,v^*)$, with u^* and v^* determined by (1) in terms of x and J_x. In this way $J(x)$ and the optimal controls $u^*(x)$, $v^*(x)$ can be constructed in the interior of a region $\mathcal{R}$ bordered by $C(x) = 0$. (If $C(x) = 0$ is a manifold of dimension $\leqq$ n-2, the terminal gradient $J_x(x_f)$ and x_f will together still involve just n-1 free parameters, and the backward construction may proceed.)

Remark. Typically, the state-space will be divided into regions $\mathcal{R}$ in which $J(x)$ is twice-differentiable, separated by "singular surfaces" across which the gradient J_x is discontinuous. The determination of such singular surfaces is crucial to the solution of most problems.

EXAMPLES:

Example 1 (cf. Isaacs [1], p. 76)

$$\begin{cases} \dot{x} = A(x,y)v - B(x,y)\sin u \\ \dot{y} = -1 - B(x,y)\cos u \end{cases} \quad , \quad |v| \leqq 1, \quad y_0 > 0$$

$C(y) \equiv y$ (the terminal surface is the x-axis); $M(x,y) =$ some $M(x)$; suppose further $0 < B(x,y) < A(x,y) < 1$, so that termination, starting with $y_0 > 0$, is assured.

$$0 = \min_{u} \max_{|v|\leqq 1} \{J_x[A(x,y)v - B(x,y)\sin u] + J_y[-1 - B(x,y)\cos u]\}$$

$$\Rightarrow \begin{cases} v^* = \operatorname{sgn} J_x \\ (\sin u^*, \cos u^*) \parallel \text{to } (J_x, J_y) \end{cases}$$

$$\Rightarrow A(x,y)|\sin u^*| = \cos u^* + B(x,y)$$

This result could have been obtained geometrically by observing that player 2 can dictate the sign of $\dot{x}$ to his advantage, and that player 1 therefore strives to minimize $|\frac{dx}{dy}|$. To do this he must choose $u = u^*$ so that (see Fig. 1) the direction $(\sin u^*, \cos u^*)$ is $\perp$ to the resultant $(\dot{x},\dot{y})$. This determines u^*:

$$A(x,y)|\sin u^*| - \cos u^* = B(x,y) \quad .$$

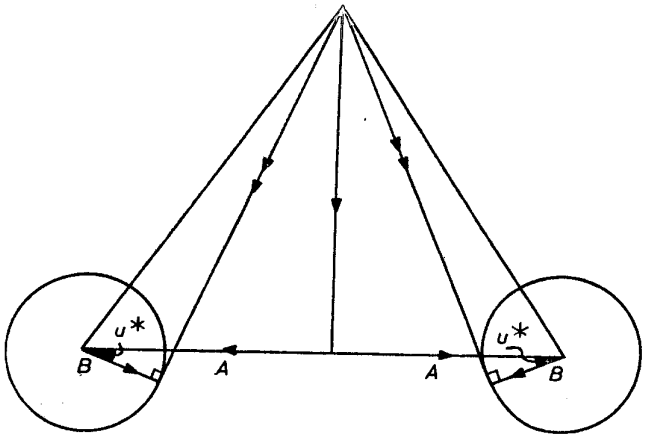

Figure 1.

On the x-axis, $J_x = M'(x)$, which determines the sign of sin u. Figures 2 a,b,c, show the general appearance of the optimal paths for various types of function M(x); in 2a, M(x) has a single minimum, and the paths move right or left according as the position lies to the right or left of a certain "dispersal line," on which player 2 can choose either direction, with player 1 reacting as soon as he becomes aware of player 2's choice. Note that, in this two-dimensional state-space, the paths <u>are</u> the "surfaces" J(x,y) = constant, and that the gradient (J_x, J_y), which determines player 2's choice of direction $(\sin u^*, \cos u^*)$, is discontinuous across the dispersal line. In Fig. 2b, M(x) has a single maximum, and there is a whole region (shaded) of positions from which player 2 can achieve Max M(x). In Fig. 2c, M(x) has one local maximum and two local minima; there are now three different dispersal lines as well as a finite region (shaded) from which player 2 secures the local maximum value of M(x).

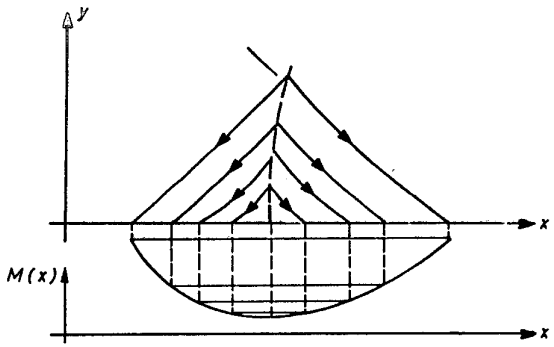

Figure 2a.

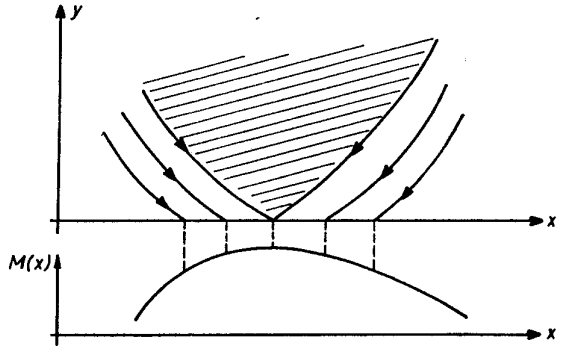

Figure 2b.

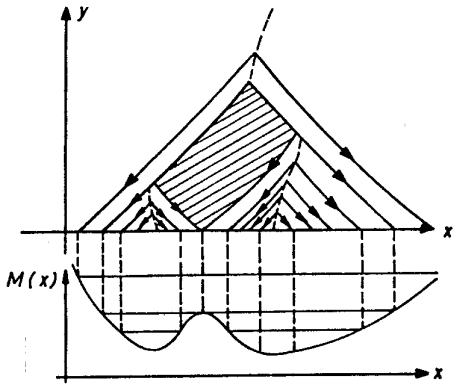

Fig 2c

Example 2 "Lady in the Lake" ([1], reprinted edition, p. 386)

$\begin{cases} P \text{ has speed } 1, \text{ confined to the perimeter of a circle, radius } R \\ E \text{ has speed } \gamma < 1, \text{ swimming inside the circle.} \end{cases}$

E wishes to land on the perimeter as far as possible from P.

Figure 3 shows the appropriate coordinate system, θ denoting the angular position of E relative to P, $(-\pi \leq \theta \leq \pi)$, and the angle ψ determines E's direction.

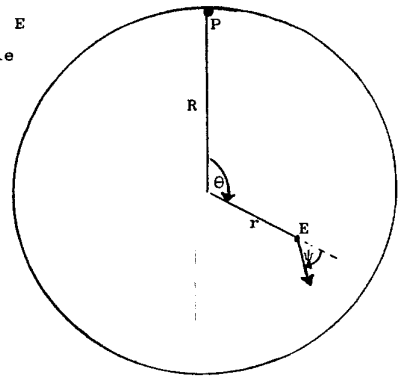

Figure 3.

$$\begin{cases} \dot{\theta} = \dfrac{\gamma \sin\psi}{r} - \dfrac{s}{R}, \quad s = \pm 1 \\ \dot{r} = \gamma\cos\psi \end{cases}$$

$$M = |\theta_f| .$$

$$0 = \min_{|s|=1} \max_{\psi} \left\{ J_r \gamma\cos\psi + J_\theta \left(\frac{\gamma\sin\psi}{r} - \frac{s}{R} \right) \right\}$$

$$\Rightarrow \begin{cases} s^* = \operatorname{sgn} J_\theta = \text{constant} = \operatorname{sgn}\theta_f \\ (\cos\psi^*, \sin\psi^*) \parallel \text{to } (J_r, \frac{1}{r} J_\theta) \end{cases}$$

$$\Rightarrow \gamma - \frac{r}{R}\sin\psi^* \operatorname{sgn}\theta_f = 0$$

Hence E runs in a straight line tangent to a circle of radius γR (see Fig. 4). This result could have been obtained geometrically by noting that E's motion in the

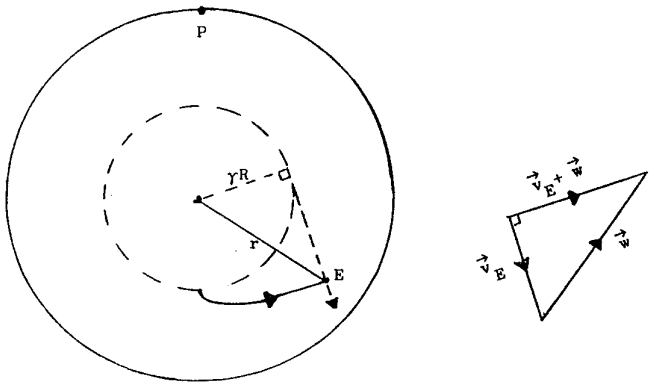

relative coordinate system attached to P is the vector sum of his own velocity $\vec{v}_E$ and a velocity $\vec{w}$ obtained by rotation about the center, opposite to P's motion, with angular velocity $\frac{1}{R}$. As in Example 1, the optimal direction for is $\perp$ to the resultant velocity $\vec{v}_E + \vec{w}$. Since $\vec{w}$ is $\perp$ to E's radius vecto and since $|\vec{v}_E| / |\vec{w}| = \frac{\gamma R}{r}$, E's velocity must be along a tangent to the γR-circl and the resultant path, whose tangent is along $\vec{v}_E + \vec{w}$, is an evolute of this circle.

This construction for E's optimal direction fails if E lies inside the γ circle. However, E can always start by moving to the relative position $\theta = \pi$ first inside and later on the γR-circle, inside of which she has angular advant Strictly speaking, E, not knowing P's instantaneous choice of direction, cann maintain $\theta = \pi$, even inside the γR-circle. However, she can keep within an arbitrarily small angle ϵ of the position $\theta = \pi$ as she moves outward toward $r = \gamma R$. From the position $r = \gamma R$, $\theta = \pi$ she then breaks right or left along the tangent. Assuming that $\gamma > .217$, she does achieve a positive terminal angular separation: $\theta_f = \pi + \operatorname{Cos}^{-1}\gamma - \frac{1}{\gamma}\sqrt{1-\gamma^2}$.

From some starting positions E can do better (see Fig. 5). The right and left evolutes intersect on $\theta = \pi$, a dispersal line. The shaded region consist of positions from which E must return to the inside of the γR-circle.

James Flynn has considered a related game "Lion and Man," with Lion, the pursuer, slower than Man, the evader, and both confined to a circular arena. In particular, if Man is constrained to remain on the perimeter of the arena [2], the problem is essentially the same as "Lady in the Lake;" E, in trying to reach the shore as far as possible from P, is in effect trying to come as close as possible to the position P' opposite to P. Now, however, the closest approach occurs before L reaches the perimeter (see Fig. 6), in fact, on the tangent from M to the γR-circle, this distance of closest approach being $D = R(\sqrt{1-\gamma^2} - \gamma\operatorname{Cos}^{-1}\gamma)$. Again, L can do better than D from some starting positions, and the cross-hatched region indicates positions which are initially closer than D but from which the distance increases immediately.

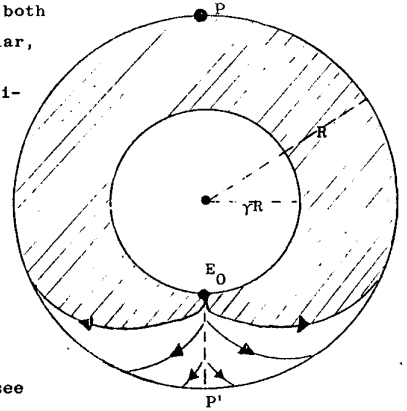

Figure 5.

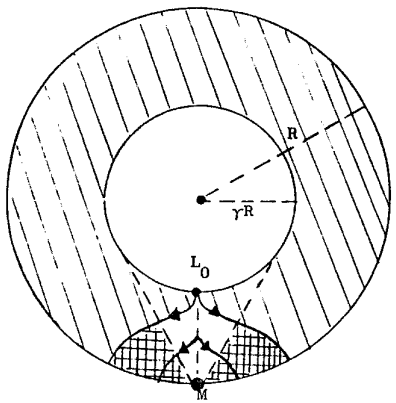

Figure 6.

Example 3 "Homicidal Chauffeur" and Related Games (in the plane)

Suppose { P has speed 1 and maximum turn-rate 1
E has speed $\gamma < 1$ and can change direction at will

P wishes to come as close as possible to E, who wishes to maximize the distance of closest approach. (This is really the "Game of Kind" in Isaacs' terminology, as opposed to the "Game of Degree" in which the payoff is the time taken to come within a specified capture distance.)

If $\vec{r}$ denotes the position of E relative to P, $\hat{u}_E$, $\hat{u}_P$ denote unit-vectors $\|$ to the motions of E,P, α denotes the direction of $\hat{u}_P$, measured from some fixed reference direction, ω_P denotes P's turn-rate, then:

$$\begin{cases} \dot{\vec{r}} = \gamma\hat{u}_E - \hat{u}_P(\alpha) \\ \dot{\alpha} = \omega_P \qquad , \quad |\omega_P| \leq 1 . \end{cases}$$

The main equation (1) becomes

$$0 = \min_{|\omega_P|\leq 1} \max_{\hat{u}_E} \left| J_{\vec{r}} \cdot (\gamma\hat{u}_E - \hat{u}_P(\alpha)) + J_\alpha \omega_P \right|$$

$$\Rightarrow \begin{cases} \hat{u}_E^* \text{ is } \| \text{ to } J_{\vec{r}} , \\ \omega_P^* = -\operatorname{sgn} J_\alpha \end{cases}$$

The adjoint equations (2) show that the gradient $J_{\vec{r}}$ is constant implying that E runs in a straight line (at least, as long as the path remains inside a region $\mathcal{R}$ in which J is twice-differentiable).

The motion can be described in a relative coordinate frame centered at P and oriented along P's direction of motion. If, in this frame, E's bearing fr P is Θ and E's heading is H (see Fig. 7), then

$$\begin{cases} \dot{r} = -\cos\Theta + \gamma\cos(H-\Theta) \\ \dot{\Theta} = \frac{\sin\Theta}{r} - \omega_P + \frac{\gamma}{r}\sin(H-\Theta) \end{cases}$$

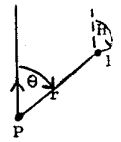

Figure 7.

The main equation in these variables shows that $\omega_P^* = \operatorname{sgn} J_\Theta$ and $H^* = \Theta + \operatorname{Tan}^{-1}(J_\Theta / rJ_r)$. ω_P^* is piecewise constant, equal to ± 1 (unless J_Θ we to remain zero for some interval of time), while H^* in this coordinate system not constant, but $(\sin H^*, \cos H^*)$ rotates at a rotate opposite to the rate ω_P of the frame.

In this game $M \equiv r$, so that at termination: $J_r = 1$, $J_\Theta = 0$, $H_f = \Theta_f$. The game ends at $\dot{r} = 0$; i.e., $C \equiv \dot{r}|_{H=\Theta} = \gamma - \cos\Theta$; hence $\Theta_f = \pm \operatorname{Cos}^{-1}\gamma$.

The paths may be constructed backwards for any final separation r_f; J_Θ i found to have the same sign as Θ_f immediately prior to termination. Hence P turns towards E who runs in a straight line which is directly away from P at closest approach. The paths of E in the relative frame may be easily construc Alternatively, we may note that the relative coordinate frame is rotating at uni angular rate, clockwise about the right turn-center C_+ or counter-clockwise about the left turn-center C_-. This angular rate is the same as in the game "Lady in the Lake" if R, there, is taken to be unity. Hence the paths in the relative frame are again evolutes of circles, now having radius γ and centered at C_+ or C_-, according as P is turning right or left ([1],[3]). This constru clearly fails if $r_f^2 + \gamma^2 > 1$. This case will be discussed later.

Figure 8 shows the paths for various r_f, with $r_f^2 + \gamma^2 < 1$, all terminati at $\Theta_f = \pm \operatorname{Cos}^{-1}\gamma$. If $r_f \leq \gamma\operatorname{Sin}^{-1}\gamma + \sqrt{1-\gamma^2} - 1$, the paths originate on the

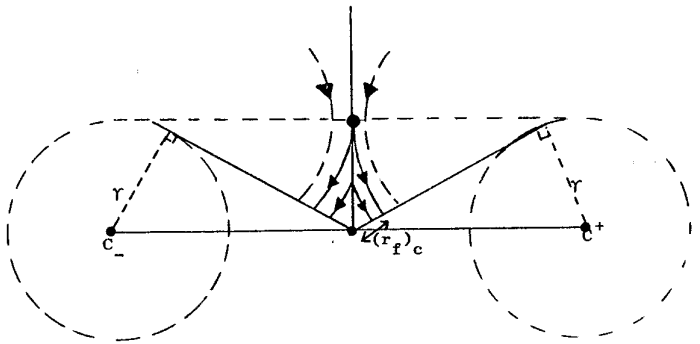

Figure 8

dispersal line $\theta = 0$, on which E has a choice as to whether to break right or left. There is a finite "capture region" corresponding to any such r_f: if E is outside this region he can prevent approach to within less than r_f, simply by running $\perp$ to the contour for this r_f whenever the relative position reaches this contour. However, E cannot prevent approach to within any r_f exceeding the critical value $(r_f)_c = \gamma \mathrm{Sin}^{-1}\gamma + \sqrt{1-\gamma^2} - 1$, since P can move E onto the line $\theta = 0$ and hold him there until $r = \gamma$ by first-of-all, if necessary, running away to sufficiently large r. $(r_f)_c$ is both the closest approach that P can achieve from all starting positions and the largest separation that E can guarantee from all starting positions except those within a finite capture region in front of P. Note that E's optimal strategy, assuming that $\theta = 0$ for $r > \gamma$, is to wait until $r = \gamma$ and then break right or left perpendicular to the relative position at this instant, at which $J_r = 0$.

Figure 9 shows the capture region for a rectangular car, assuming a typical relatively large turn-radius.

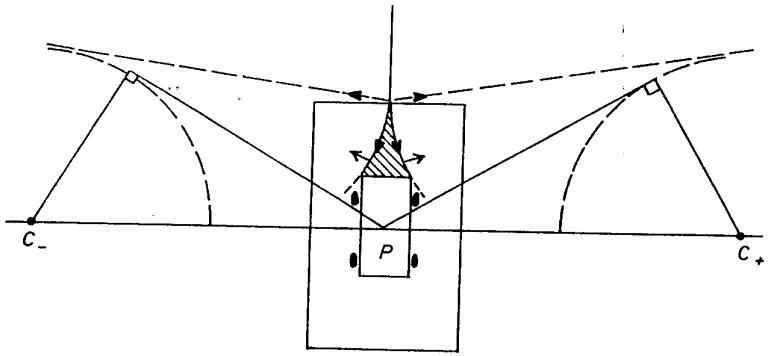

Figure 9.

Figure 10 shows the capture region for a similar rectangular car for the gam "Suicidal Pedestrian," in which E is now trying to be captured and P to prev capture. ω_P is now $-J_\theta$, but J_θ changes sign from + to - shortly before termination of the grazing path at a rear corner of the car; P turns initially away from E, but near termination he turns towards E to prevent the rear corn of the car from striking P.

Figures 11 a,b,c show the Surveillance Region in the game "Surveillance Evasion" [4], in which P strives to minimize the maximum separation r_f and E to maximize it. The Surveillance Region, for given r_f, indicates those positions from which the maximum separation does not exceed r_f, so that P can keep E within a surveillance range r_f. Figure 11a is applicable if $f_3(\gamma) \triangleq 1 + \sqrt{1-\gamma^2} + \gamma(\pi + \mathrm{Sin}^{-1}\gamma) < r_f$. Figure 11b is applicable if $f_2(\gamma) \triangleq \sqrt{1-\gamma^2} + \gamma(\pi + 2\mathrm{Sin}^{-1}\gamma) < r_f < f_3(\gamma)$. Here J_θ changes sign at the point and the right barrier, for example, starts with a left turn by P, followed at by a right turn.

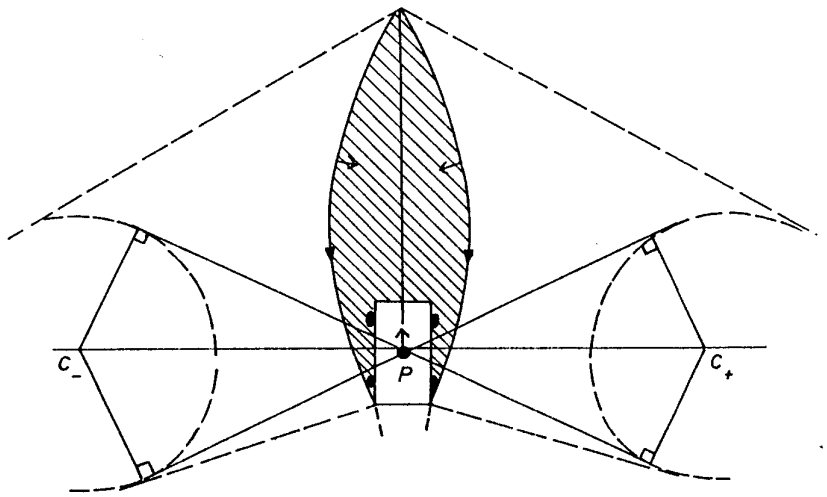

Figure 10.

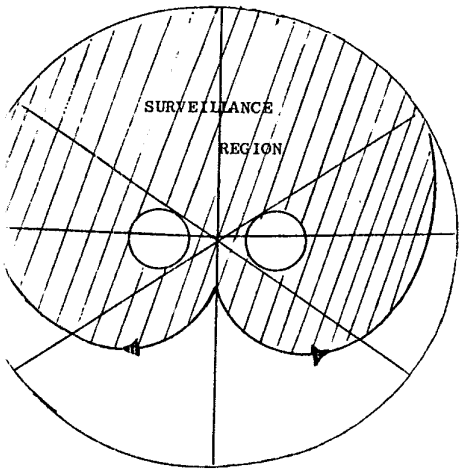

Figure 11a.

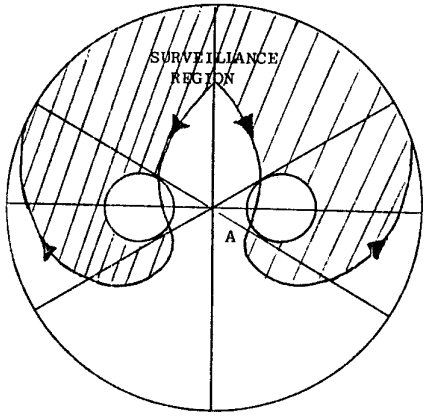

Figure 11b.

$\sqrt{1-\gamma^2} + \gamma(1 + \frac{\pi}{2} - 2\mathrm{Sin}^{-1}\gamma) < r_f < f_2(\gamma)$, the Surveillance
llustrated in Fig. 11c. Here P's left turn is followed
but the barrier direction is now discontinuous at B.
ro as the path approaches B (in forward time), E cannot
osite barrier [5].

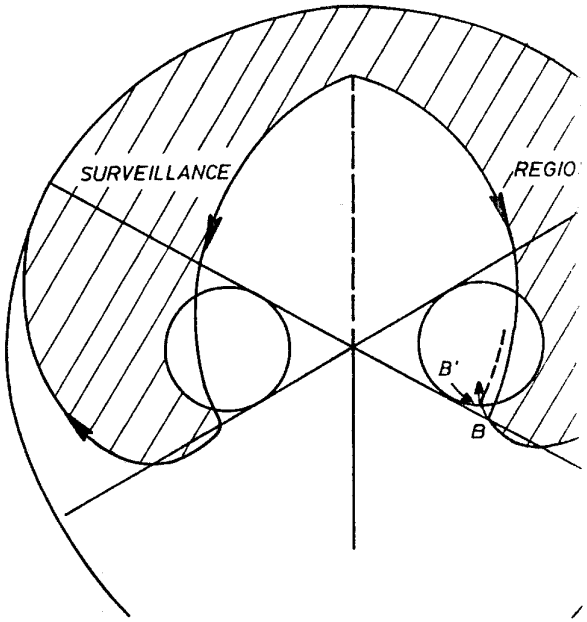

Figure 11c.

If, on the other hand, we attempt to define a larger Surve
bounded by a composite with a corner at B' in Fig. 11c, so tha
a switch to a right turn by P, together with a continuation of
⊥ to the arriving barrier, will lead to $\frac{d}{dt}(J^-) > 0$ and $\frac{d}{dt}$
a direction at B' (indicated by a dotted arrow) leading to es
for Surveillance Region.

Returning to the "Homicidal Chauffeur" game, we look final
when $r_f^2 + \gamma^2 > 1$. It follows from the main equation that as
$J_\theta \to 0$ or $\dot{\theta} \to 0$. As shown by Isaacs [1], it is not possible
with $[J_\theta]_{t_f} = 0$ if $r_f^2 + \gamma^2 > 1$, since this leads to $\ddot{r}|_{t_f} <$
therefore, the terminal condition is one of relative equilibriu
positive θ_f, for example, this requires $H_f > \theta_f > \mathrm{Cos}^{-1}\gamma$. I
configuration, P and E are describing concentric circles, a
rate, of radii 1 and γ respectively. The critical capture
moreover, is again reached by E running ⊥ to the initial pc
$\theta = 0$, since E optimizes the range for his initial break to
implying that J_r is initially zero. Figure 12 shows the path
in this case: E has moved unit distance in reaching equilib

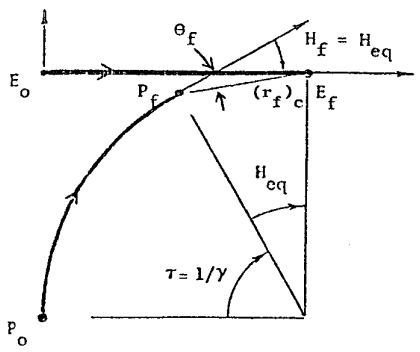

Figure 12.

Example 4 "Game of Two Cars" ([1], p.237)

Here the evader of E of example 3 also has a maximum turn-rate, say ω, with $\omega > 1$. The heading H now becomes a third state variable, and the complete equations are:

$$\begin{cases} \dot{r} = -\cos\theta + \gamma\cos(H-\theta) \\ \dot{\theta} = \dfrac{\sin\theta}{r} - \omega_P + \dfrac{\gamma}{r}\sin(H-\theta) \\ \dot{H} = \omega_E - \omega_P \end{cases}, \qquad \begin{cases} (\omega_P) \leqq 1 \\ (\omega_E) \leqq \omega \end{cases}.$$

The optimal turn-rates are $\omega_P^* = \text{sgn}(J_\theta + J_H)$, $\omega_E^* = \omega\ \text{sgn}\ J_H$ as long as $J_\theta + J_H$ and J_H do not remain zero. The optimal paths of example 3, for which $\omega_E = 0$ and $\omega_P = \pm 1$, are again optimal, being now "singular arcs" along which J_θ remains zero. However, from most initial states (r,θ,H) a singular arc must be preceded by a "tributary arc" on which $|\omega_E| = \omega$.

In particular, the critical capture radius is now reduced to

$$(r_f)_c = \gamma\ \text{Sin}^{-1}\gamma + \sqrt{1-\gamma^2} - 1 - \frac{\gamma}{\omega}\left(\frac{\pi}{2} - 1\right)$$

If (case I) this doesn't exceed $\sqrt{1-\gamma^2}$, as is evident from Fig. 13; E loses time in turning from a neutral initial heading $H = 0$ or $H = \pi$ towards his optimal direction which is again perpendicular to the initial relative position.

If $(r_f)_c$ exceeds $\sqrt{1-\gamma^2}$ (case II) the situation shown in Fig. 12 must be similarly modified, as shown in Fig. 14. The critical capture radius is now:

$$(r_f)_c = \sqrt{1 + \gamma^2 - 2\gamma\ \sin\left|\frac{1}{\gamma} + \left(\frac{\pi}{2} - 1\right)/\omega\right|}\ .$$

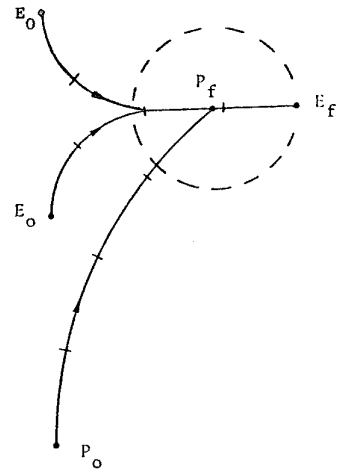

Figure 13 Critical Trajectories in Region I

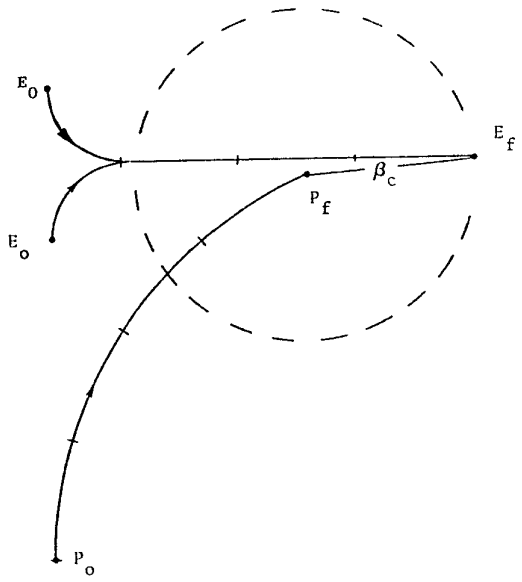

Figure 14 Critical Trajectories in Region II

Finally, if $\frac{1}{\omega} \leq \gamma < \sin\frac{\pi}{2\omega}$ (Case III), the minimum range occurs while E is still turning toward his optimal direction, i.e., there is no singular arc, and the following equations hold (see Fig. 15):

$$(r_f)_c + 1 - \cos\tau = \frac{\gamma}{\omega}(1 - \cos\omega\tau)$$

$$\sin\tau = \gamma \sin\omega\tau \quad ,$$

Since $\dot{r}_f = 0$ and, as in Case I, $J_\theta)_{t_f} = 0$, $H_f = \theta_f$, and the final relative position is perpendicular to the initial one.

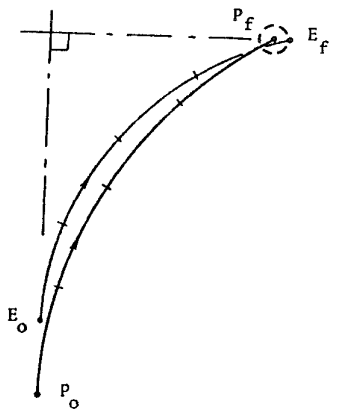

Fig. 15 Critical Trajectories in Region III

Note that as the product $\gamma\omega$, which is E's lateral acceleration, approaches 1, which is P's lateral acceleration, $\tau \to 0$ and $(r_f)_c \to 0$. This agrees with a result due to Cockayne [6], proving that $\frac{\gamma}{\omega} \leq 1 \rightarrow (r_f)_c = 0$.

Contours of constant $(r_f)_c$ are shown in a parameter space $(\gamma, \frac{1}{\omega})$ in Fig. 16. These contours pass smoothly in and out of all 3 regions I, II, III.**

It remains to demonstrate that $(r_f)_c$ corresponds to the largest closed "barrier" $J(r,\theta,H)$ = constant. Backwards construction of all the optimal paths, terminating with $r = (r_f)_c$, and with $H_f = \theta_f$ or $H_f \neq \theta_f$ (no singular arc), reveals that the surface formed by these paths does not reach the symmetry plane $\theta = 0$ except at the neutral headings $H = 0$ and $H = \pi$. This is illustrated by 3 sections of this barrier surface shown in Figs. 17 a,b,c.

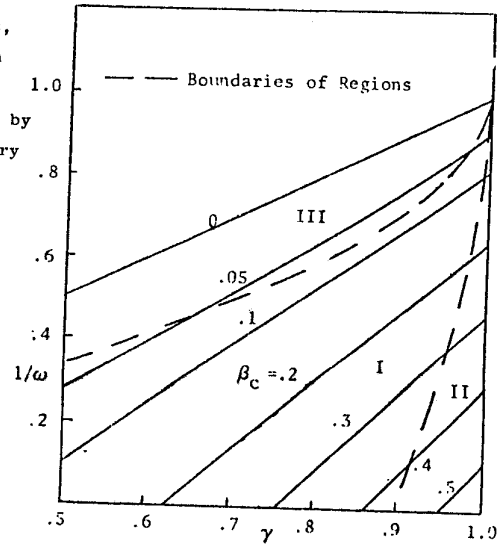

Fig. 16 Variation with Speeds and Turn

** entirely equivalent analysis has been carried out by S. Sharma and T. Miloh, not yet published.

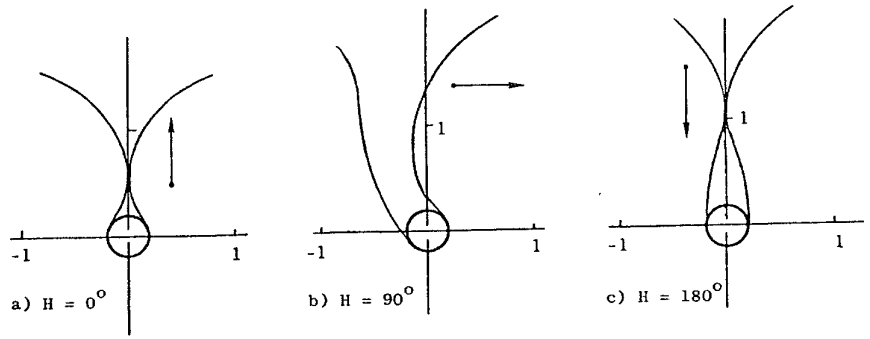

Fig. 17 Appearance of Barrier for Parameters in Region I

The barrier must be closed, at headings other than $H = 0$ and π, by finding those initial states from which E can barely return to a neutral heading $H = 0$ or π before it is "too late." Thus if E wishes to return to $H = 0$, P will reduce θ to zero and E must reach a heading $H = 0$ before r falls below $\gamma - \frac{\gamma}{\omega}$. This constitutes a preliminary game terminating at $H = 0$, $\theta = 0$, for which the terminal gradient (J_r, J_θ, J_H) is no longer unique, and the critical trajectories end at $r = \gamma - \frac{\gamma}{\omega}$. The paths of this preliminary game may be constructed backwards and P's strategy can be quite complex (see ref. [7]). After reaching the decision point $(\gamma - \frac{\gamma}{\omega}, 0, 0)$ E then decides whether to break right or left. A similar situation arises if E wishes to return to the "head-on" decision point $(\gamma + \frac{\gamma}{\omega}, 0, \pi)$. Naturally E chooses the more accessible of the two decision points, and from points on the critical barrier he can barely reach one of them. Typical composite barrier sections are shown in Figs. 18 a,b,c. The edges of the

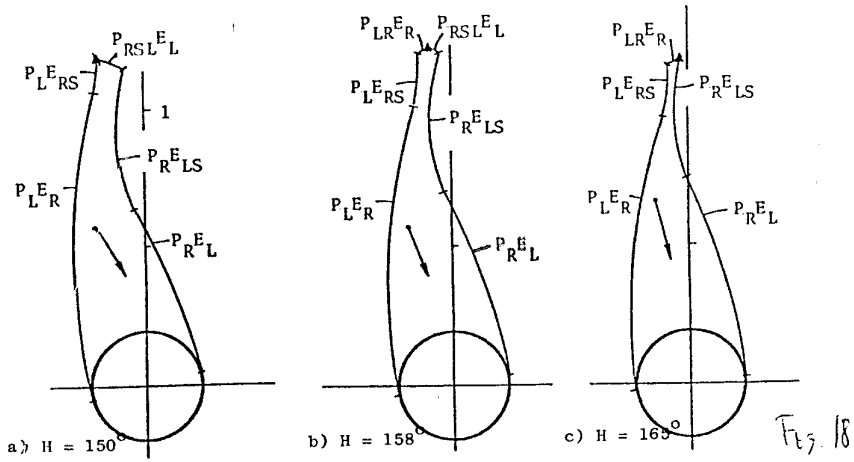

Fig. 18

of the composite barrier are either dispersive (marked ▲ in Figs. 18) or constitute the paths themselves, so that Bernhard's conditions are met [5].

A more complicated barrier in a game with identical equations of motion occurs in the "Role Determination" problem in which one airplane can destroy another if the latter comes directly in front of the former. A composite barrier separates states (r,θ,H) leading to victory by one or the other. Space does not permit further discussion of this interesting problem, but it is described in ref. [8].

Example 5 The "Deadline Game" ([1], p. 265) and related problems.

For what initial positions of pursuer P (speed 1) and evader E (speed $w > 1$) can E pass between P and the x-axis (see Fig. 19), moving in the positive x-direction without coming closer to P than a specified distance ℓ ? The answer to this "game of kind" is obviously obtainable if we can solve the following equivalent "game of terminal payoff:" What is the distance ℓ of closest approach from any given starting position, assuming that P minimizes ℓ and E maximizes ℓ while passing between E and the x-axis?

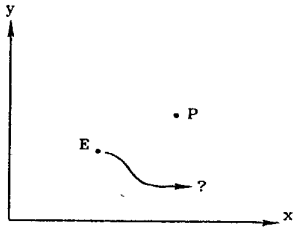

Figure 19

The positions corresponding to any particular value of ℓ will lie on a surface in the 3-dimensional state-space (x,y_P,y_E), where x denotes x_P-x_E, and the limiting surface as $\ell \to 0$ can be obtained by purely geometrical reasoning: $\ell > 0$ provided that the Apollonius circle (of positions which E can reach before P) does not reach the x-axis. As $\ell \to 0$ this circle must tend to tangency with the x-axis (Fig. 20); i.e., $y_c \to \sqrt{(EC)(PC)}$. But $y_c = y_P + \frac{y_P-y_E}{w^2-1}$ and $\frac{EC}{w^2} = \frac{PC}{1} = \frac{EP}{w^2-1}$. Hence, in the limit, $w^2 y_P - y_E = w(EP)$,

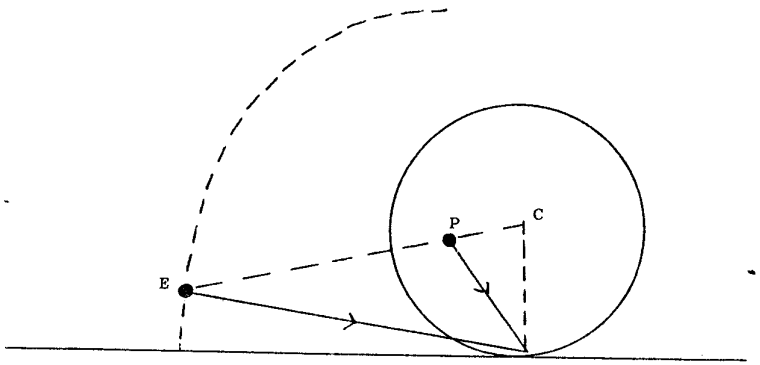

Figure 20

which defines an ellipse, eccentricity $1/w$, focus at P and minor axis along the x-axis (dotted in Fig. 20).

For $\ell > 0$, Isaacs analyzes the optimal paths in this game and concludes that they have two phases: a first, straight-line phase during which the distance PE is decreasing, and a second, curved, phase during which the distance PE remains equal to ℓ. The second phase terminates with E's path tangent to the x-axis at E_f and P, now at P_f, moving directly towards E_f (see Fig. 21) after which the distance PE increases. P's curved path is determined by the maximization of $-\frac{dy_E}{d\theta}$ subject to PE = ℓ, which determines, in turn, E's curved path. The first phase straight paths are tangent to the second phase curved paths.

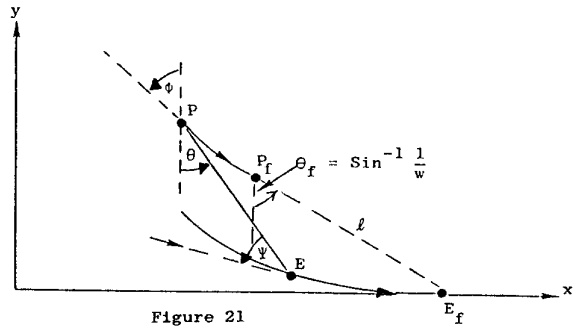

Figure 21

To verify these features, let $J(\vec{r}_E,\vec{r}_P)$ denote the closest approach distance ℓ corresponding to initial positions $\vec{r}_E$ and $\vec{r}_P$ of E and P, respectively. If $\hat{\beta}_E$ and $\hat{\beta}_P$ denote unit-vectors parallel to the velocities of E and P respectively, the main equation is:

$$0 = \operatorname*{Max}_{\hat{\beta}_E} \operatorname*{Min}_{\hat{\beta}_P} \left(J_{\vec{r}_E} \cdot w\hat{\beta}_E + J_{\vec{r}_P} \cdot \hat{\beta}_P \right)$$

$$= w\left| J_{\vec{r}_E} \right| - \left| J_{\vec{r}_P} \right| ,$$

with $\hat{\beta}_E$, $\hat{\beta}_P$ parallel to $J_{\vec{r}_E}$, $-J_{\vec{r}_P}$ respectively.

The gradient vectors $J_{\vec{r}_E}$, $J_{\vec{r}_P}$ are, furthermore, constant along unconstrained paths, implying straight-line motion. Moreover, $J(\vec{r}_E,\vec{r}_P)$ is a function $J(x,y_P,y_E$ where $x = x_P-x_E$, so that $J_{x_E} = -J_{x_P}$. It now follows that the "controls" Ψ,Φ (see Fig. 21) satisfy:

$$\frac{w}{\sin \Psi} = \frac{1}{\sin \Phi} \qquad (A)$$

During the final phase, however, E must observe the "state constraint" that EP not be allowed to decrease further. This requires that E's control Ψ be a function $\tilde{\Psi}(\phi,\theta)$ defined by

$$w\cos(\Psi-\theta) = \cos(\phi-\theta) \quad . \tag{B}$$

[If an objection is raised to this implicit assumption that E knows P's present control ϕ, E can achieve as small a change in EP as he pleases by utilizing knowledge of P's control in the recent past, as close as necessary to the present.]

The constrained main equation, using coordinates r,θ,y_E in place of x,y_P,y_E where $r = EP$, is:

$$\min_{\substack{\phi \\ \Psi=\tilde{\Psi}(\phi,\theta)}} \left(J_\theta \dot{\theta}(\theta,\phi,\tilde{\Psi}) + J_{y_E}\dot{y}_E(\theta,\phi,\tilde{\Psi})\right) = 0 \quad ,$$

which implies the stationarity of $\frac{dy_E}{d\theta}$ w.r.t.ϕ. [Obviously, $-\frac{dy_E}{d\theta}$ should be maximized.] It is also easily verified, by comparing constrained and unconstrained main equations in coordinates r,θ,y_E, that Ψ and ϕ must be continuous at junctions of the unconstrained and constrained paths. This proves that the unconstrained paths are straight tangents to the second phase curved paths. The curved path directions Ψ,ϕ are determined by (A) and (B) (see [9]) and it is shown in [1] equation (9.5.9) that the resulting paths, for given ℓ, are given by

$$\left.\begin{aligned} y_E &= \frac{\ell}{w^2-1}(kw - w\theta - w^2\cos\theta) \\ y_P &= \frac{\ell}{w^2-1}(kw - w\theta - \cos\theta) \\ x_E &= \frac{\ell}{w^2-1}(w^2\sin\theta - w) + x_{E_f} \\ x_P &= \frac{\ell}{w^2-1}(\sin\theta - w) + x_{E_f} \end{aligned}\right\} ,$$

where $k = \sqrt{w^2-1} + \mathrm{Sin}^{-1}\frac{1}{w}$.

These paths may be constructed geometrically by rolling the Apollonius circle, now of radius $w\ell/(w^2-1)$, along a line through E_f parallel to the y-axis (see Fig. 22). Indeed, the instantaneous center of rotation of the frame, rigidly attached to E and P during the curved phases, must lie on this Apollonius circle. P, wishing to maximize $-\frac{dy_E}{d\theta}$ where θ measures the orientation of this frame, chooses the instantaneous center as far to the right as possible in Fig. 22. Hence the above geometrical construction.

The inclusion of the first phase straight tangents gives $y_P(\theta,\tau)=y_P(\theta)-\tau y_P'(\theta)$, etc., as in [1], equation (9.5.10). This expresses $y_E, y_P, x_E-x_{E_f}, x_P-x_{P_f}$ in terms of ℓ,θ,τ :

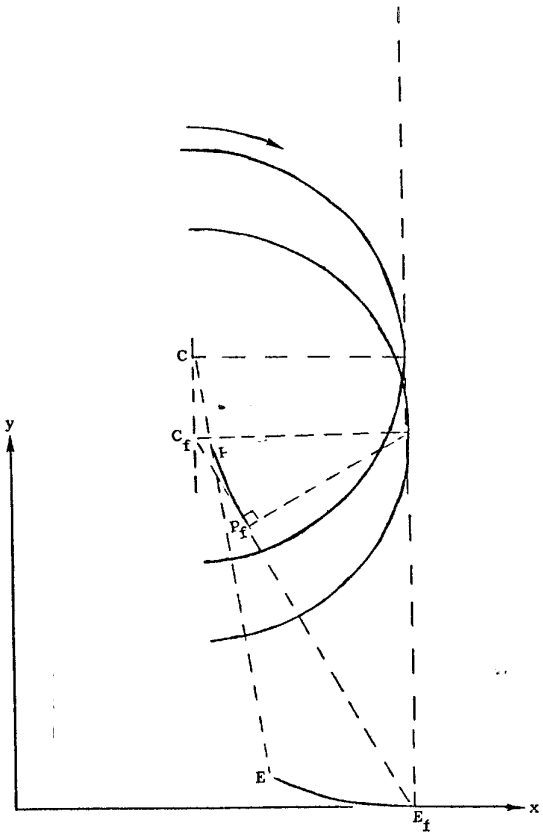

Figure 22.

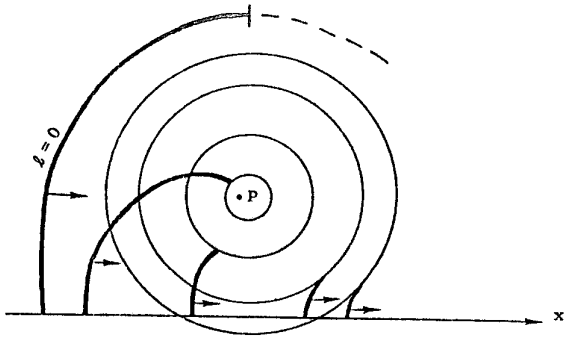

Figure 23.

$$\left.\begin{aligned} y_E &= \frac{\ell}{w^2-1}\left\{kw - w\theta - w^2\cos\theta + w\tau(1 - w\sin\theta)\right\} \\ y_P &= \frac{\ell}{w^2-1}\left\{kw - w\theta - \cos\theta + \tau(w - \sin\theta)\right\} \\ x_E &= \frac{\ell}{w^2-1}\left\{w^2\sin\theta - w - w^2\tau\cos\theta\right\} + x_{E_f} \\ x_P &= \frac{\ell}{w^2-1}\left\{\sin\theta - w - \tau\cos\theta\right\} + x_{E_f} \end{aligned}\right\}$$

A section, for fixed y_P, of the surfaces corresponding to various ℓ, is sketched in Fig. 23, E's optimal direction, indicated by arrows, being perpendicular to the local ℓ-contour.

A somewhat similar problem arises if E wishes to pass between two slower pursuers. Again the final phase is one of curved motion, in this case by E and the closer pursuer, and the state-space is again essentially 3-dimensional. Space does permit further elaboration, but the complete solution appears in reference [10]. Appendix A lists certain errata in reference [10].

Returning to the deadline game, suppose that E is permitted to escape in either direction along the x-axis. This is the two-sided deadline game, [1], p. 260. Figure 24 shows a section of the surfaces S_1, S_2 corresponding to a fixed y_P and a single value of ℓ, and to escape to the right, left respectively. The surfaces S_1, S_2 in the 3-dimensional state-space (x, y_P, y_E) intersect along a "dispersive edge," designated by (D) in Fig. 24, with the following property: if E at (D) chooses, for example, to escape to the right, he will remain on S_1 but will move off of surface S_2 to the "capture" side, i.e., he will no longer be in a position to escape to the left.

The surfaces S_1, S_2, together with their junction (D), form a composite

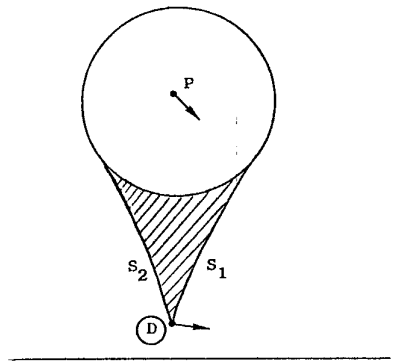

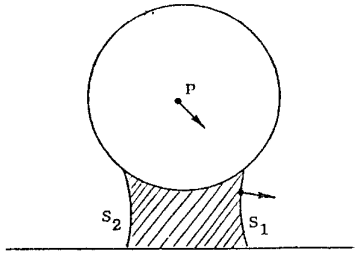

Figure 24.

escape (without coming closer to P than ℓ). Analytically this is expressed by $J^{(2)}_{\vec{r}_E} \cdot w\hat{\beta}_E^{(1)} + J^{(2)}_{\vec{r}_P} \cdot \hat{\beta}_P^{(1)} < 0$ at (D), which, because of the main equation, may be expressed in the symmetric form:

$$\hat{\beta}_E^{(1)} \cdot \hat{\beta}_E^{(2)} - \hat{\beta}_P^{(1)} \cdot \hat{\beta}_P^{(2)} < 0 \text{ at } (D) .$$

Patrolling a Channel

An interesting extension of the one-sided deadline game is the game: "patrollin a channel," also discussed in [1]. Here E can choose whether to pass along the channel (to the right in Fig. 25) above or below P. If the width L of the channel is less than a critical width:

$$L_c = \frac{2\ell w}{w^2-1}\left(\frac{\pi}{2} + k\right) ,$$

the surfaces S_1 and S_2, corresponding to passage below or above P respectively, form with the ℓ-circle around P the boundary of a capture region (shaded).

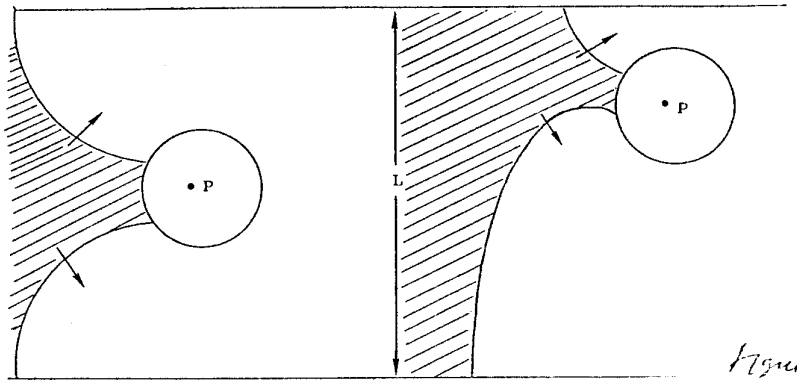

Figure 25

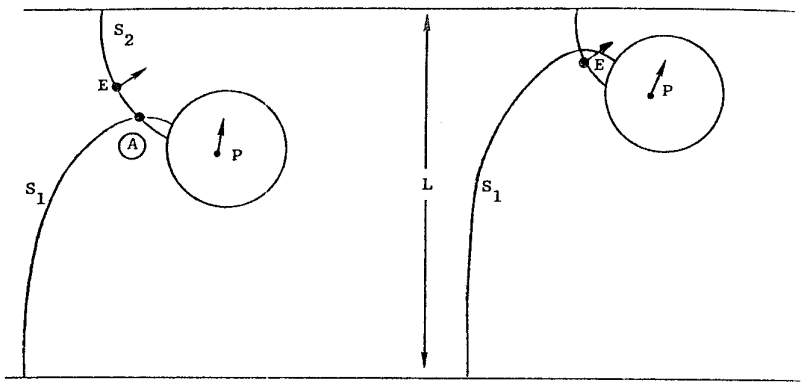

Figure 26.

If, however, $L > L_c$, the surfaces S_1 and S_2 intersect outside the ℓ-circ in an "attractive edge," designated by A (see Fig. 26), which is such that if, for example, E chooses to pass above P, E remains on S_2 but moves off of S_1 to the escape side, i.e., $\hat{\beta}_E^{(1)} \cdot \hat{\beta}_E^{(2)} - \hat{\beta}_P^{(1)} \cdot \hat{\beta}_P^{(2)} > 0$ at (A). The surfaces S_1 and S_2 thus clearly fail to form a composite semi-permeable surface -- if P guards against passage above P, E can pass below P.

The Cornered Rat

A further extension is the "cornered rat" game, also mentioned by Isaacs in [1 The state-space is now essentially 4-dimensional and the locus of E's positions for fixed P, corresponding to given ℓ and to escape along the x or y directi is sketched in Figs. 27 a,b,c. For P sufficiently close to the corner, as in Fig. 27a, the hypersurfaces S_1 and S_2 do not intersect. For P somewhat further from the corner they intersect in two "dispersal hyperedges," denoted by (D) in Fig. 27b. But for P sufficiently far from the corner, as in Fig. 27c, S_1 and S_2 intersect in an "attractive hyperedge" (A). The hypersurfaces thus again fail to combine into a composite semi-permeable hypersurface.

The critical positions P^* and E^*, corresponding to a change from dispersive

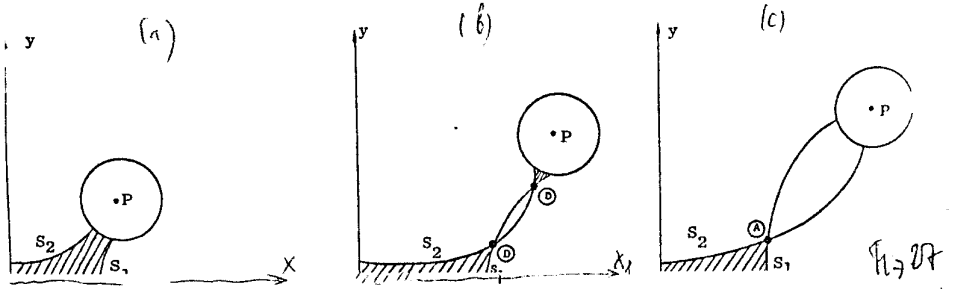

Fig 27

yperedge (D) to attractive hyperedge (A), satisfy:

$$\hat{\beta}_E^{(1)} \cdot \hat{\beta}_E^{(2)} - \hat{\beta}_P^{(1)} \cdot \hat{\beta}_P^{(2)} = 0 \ .$$

is straightforward to verify that this implies: $\tau_1 = \tau_2 = 1$ and $\theta_2 = -\theta_1$ being measured from the x-axis rather than the y-axis), and that the P^*- and -loci, sketched in Fig. 28, are given by:

$$\left.\begin{aligned}
\frac{w^2-1}{\ell} x_P^* &= kw + w\theta_1 - \cos\theta_1 + w + \sin\theta_1 \\
\frac{w^2-1}{\ell} y_P^* &= kw - w\theta_1 - \cos\theta_1 + w - \sin\theta_1 \\
\frac{w^2-1}{\ell} x_E^* &= kw + w\theta_1 - w^2\cos\theta_1 + w + w^2\sin\theta_1 \\
\frac{w^2-1}{\ell} y_E^* &= kw - w\theta_1 - w^2\cos\theta_1 + w - w^2\sin\theta_1
\end{aligned}\right\}$$

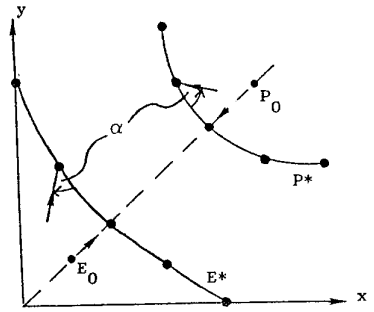

Figure 28.

It may further be easily verified that $P^*E^* = \ell\sqrt{2}$ and the arc-lengths of these loci satisfy $|d\vec{r}_E^*| = w|d\vec{r}_P^*|$. We anticipate that for positions P outside of the P^*-locus there is a locus of positions E inside the E^*-locus from which P and E move in straight lines towards a decision surface consisting of the P^*- and E^*-loc for various ℓ, at which time E chooses which side of P to pass. If so, the directions during the "delayed option" phase of the game are determined by:

$$0 = \frac{dV^*}{d\theta_1} = J^{(3)}_{\vec{r}_E} \cdot \vec{r}_E^{*\prime}(\theta_1) + J^{(3)}_{\vec{r}_P} \cdot \vec{r}_P^{*\prime}(\theta_1) \ ,$$

which may be rewritten:

$$\hat{\beta}_E^{(3)} \cdot \vec{r}_E^{*\prime}(\theta_1) - w\hat{\beta}_P^{(3)} \cdot \vec{r}_P^{*\prime}(\theta_1) = 0 \ ,$$

the superscript (3) denoting the delayed-option phase. Together with the arc-length relation this implies that the delayed-option phase straight paths make equal angles each say α, with the E^*- and P^*-loci, as indicated in Fig. 28. In particular, for the symmetric positions E_0 and P_0 the two players move directly toward

ıer before E decides which way to pass.
e locus of positions E corresponding to
lelayed option strategy, when P is
:side the P^*-locus, can now be computed.
;ure 29 shows a sketch of how this locus
)uld look. Note that the last equation
page 24 is satisfied automatically by
$(\hat{\beta}_E^{(3)},\hat{\beta}_P^{(3)}) = (\hat{\beta}_E^{(1)},\hat{\beta}_P^{(1)})$, i = 1 or 2,
ıce $(\vec{r}_E^*(\theta_1), \vec{r}_P^*(\theta_1))$ belongs to both
)ersurfaces S_1 and S_2 for all θ_1.
e surface S_3 thus joins smoothly
:o the surfaces S_1 and S_2.

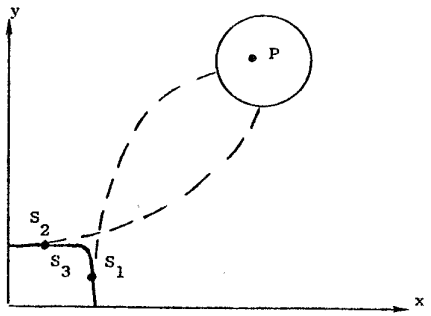

Figure 29.

;ure 29 replaces Fig. 27c and, together with Figs. 27 a,b, defines a composite
·rier. Note that on the E^*- and P^*-loci the quantities
$\cdot w\hat{\beta}_E^{(3)}(\alpha) + \vec{J}^{(1)}\cdot\hat{\beta}_P^{(3)}(\alpha)$, i = 1 and 2, which are homogeneous linear in $\sin\alpha$
$\vec{r}_P$
$\cos\alpha$, vanish for two distinct α's not differing by π, and therefore vanish
ntically. The delayed-option paths thus arrive tangentially to both hyper-
faces S_1 and S_2, thus fulfilling necessary conditions described in [5].

FERENCES

Isaacs, R., Differential Games, Wiley 1966 and Krieger, 1975.

Flynn, J., "Lion and Man: The Boundary Constraint," SIAM J. Contr. 11 (1973), 397-411.

Lewin, J. and J.V. Breakwell, "The Surveillance-Evasion Game of Degree," JOTA, 16, Nos. 3/4, (Aug. 1975), 339-353.

Dobbie, J.M., "Solution of Some Surveillance-Evasion Problems by the Methods of Differential Games," Proc. 4th Internat'l. Conf. on Operational Research, MIT, (Wiley, 1966).

Bernhard, P., "Conditions de Coin pour les Jeux Differentiels," Seminaire sur les Jeux Differentiels, Centre d'Automatique, Paris (1971).

Cockayne, E., "Plane Pursuit with Curvature Constraints," SIAM J. Appl. Math., Vol. 15, No. 6, Nov. 1967, pp. 1511-1516.

Breakwell, J.V. and A.W. Merz, "Minimum Required Capture Radius in a Coplanar Model of the Aerial Combat Problem," submitted to AIAA Journal for publication.

Olsder, G.J. and J.V. Breakwell, "Role Determination in an Aerial Dogfight," Int. J. of Game They., Vol. 3, Issue 1, pp. 47-66, 1974.

Breakwell, J.V., "Pursuit of a Faster Evader," The They. & Appl. of Diff. Games, pp. 243-256, 1975.

Hagedorn, P. and J.V. Breakwell, "A Differential Game with Two Pursuers and One Evader," JOTA, Vol. 18, No. 1, Jan 1976

APPENDIX A ERRATA IN REFERENCE [10]

Page 446, eq'n. (14): $\dot{\theta} = \dot{\phi}_1 + [ws/2\sqrt{1-w^2c^2}\,\dot{\phi}_1]$

Page 449, eq'n. (27): delete the terms $-2sc\tau$

Page 449, eq'n. (29), 2nd line: $+ (2c^2-1)\tau$

Page 449, eq'n. (31), left member: $y_{P_2}(\phi_1,\tau) = \ldots$

Page 451, eq'n. (33): replace each z_r by z_r^2